Engineering Geology 160 (2013) 1–7

Contents lists available at SciVerse ScienceDirect

Engineering Geology

journal homepage: www.elsevier.com/locate/enggeo

Dynamic response of a rock fracture filled with viscoelastic materials

W. Wu [a,*], J.B. Zhu [b], J. Zhao [a]

[a] Ecole Polytechnique Fédérale de Lausanne (EPFL), School of Architecture, Civil and Environmental Engineering, Laboratory of Rock Mechanics (LMR), CH-1015 Lausanne, Switzerland
[b] Graduate Aeronautical Laboratories and Department of Mechanical and Civil Engineering, California Institute of Technology, Pasadena, CA 91125, USA

ARTICLE INFO

Article history:
Received 30 November 2012
Received in revised form 18 March 2013
Accepted 30 March 2013
Available online 8 April 2013

Keywords:
P-wave propagation
Filled rock fracture
Specific initial mass
Specific fracture stiffness
Wave transmission coefficient

ABSTRACT

Rock fractures filled with viscoelastic materials, such as sand, usually contribute to rock mass instability under the influence of seismic waves and dynamic loads. The purpose of this study is to verify that the specific fracture stiffness and the specific initial mass of the filling sand are two key fracture parameters in interrelating the physical, mechanical and seismic properties of a rock fracture filled with dry sand. A series of dynamic tests using a split Hopkinson rock bar was conducted on a simulated sand-filled fracture. The experimental results show that stress wave attenuation across the filled fracture is strongly affected by wave reflection and transmission at the fracture interfaces and the dynamic compaction of the filling sand. With the comparison between the analytical predictions by the displacement discontinuity model and the displacement and stress discontinuity model and the experimental results from the laboratory tests, it is found that both models can predict a filled fracture with a smaller thickness (i.e., less than 10 mm). The displacement and stress discontinuity model may be used to predict a fracture with a larger thickness by considering the specific initial mass of filling materials. The wave transmission coefficient for a filled fracture generally increases with increasing specific fracture stiffness.

1. Introduction

Rock fractures, including the non-welded contact and filled fractures, universally exist in rock masses. Fracture displacement (e.g. opening, closure, and slip) has long been recognized as resulting in rock mass instability (Zhao, 1997; Indraratna et al., 2010). When stress waves propagate across fractured rock masses, fractures are commonly considered as displacement discontinuity boundaries (Schoenberg, 1980; Cai and Zhao, 2000). Each fracture is treated as a non-welded contact with negligible thickness compared with the incident wavelength. The specific fracture stiffness is the link parameter between continuous stresses and discontinuous displacements.

Although the displacement discontinuity model (DDM) has been widely adopted to investigate the dynamic response of a rock fracture, it may be imprecise to study a fracture filled with viscoelastic materials, such as weathered rock, sand and clay. Rokhlin and Wang (1991) used a mass per unit area of filling materials in the boundary conditions of two solid semi-spaces separated by a viscoelastic layer. The stress across the filling layer thus becomes discontinuous, due to the viscoelasticity that expressed by an imaginary part in the elastic constants. Meanwhile, the thickness of filling materials may not be overlooked compared with the wavelength. A newer and more precise model to describe the boundary conditions of a filled fracture, the displacement and stress discontinuity model (DSDM), has been developed by Zhu et al. (2011). It proposes that the stress discontinuity across a filled fracture is caused by the specific initial mass of filling materials and the displacement discontinuity is determined by the transmitted stress and the specific fracture stiffness.

There are many experimental methods to investigate stress wave generation and propagation across artificial rock fractures, such as an ultrasonic wave (Zhao et al., 2006a; Li and Zhu, 2012) and a pendulum hammer (Leucci and Giorgi, 2006; Li and Ma, 2009). In this study, a split Hopkinson rock bar (SHRB) apparatus (Wu et al., 2012, 2013) was used to study the effects of fracture properties and loading conditions on the dynamic response of a rock fracture filled with dry sand. The advantages of this technique include the following: (1) characterization of the interaction between a stress wave and rock fractures; (2) observation of a low-frequency wave generation and propagation in a rock medium; (3) measurement of the stress–time responses of fracture interfaces independently, considering dynamic stress non-equilibrium across a filled fracture. Furthermore, the low tensile strength of rock materials can withstand a low loading rate impact, which is suitable for the study of stress wave propagation across rock fractures. A high loading rate impact is usually provided by a conventional split Hopkinson pressure bar (SHPB) (Wu et al., 2010; Chen and Song, 2011), which may induce fracturing and fragmentation of rock materials. It is thus unnecessary to consider the fracture response and should focus on the material behavior.

The purpose of this study is to verify that the specific fracture stiffness and the specific initial mass of filling materials interrelate the physical, mechanical and seismic properties of a fracture filled with viscoelastic materials. The fracture thickness is a fracture physical property, the

* Corresponding author. Tel.: +41 216933962; fax: +41 216934153.
E-mail address: wei.wu@epfl.ch (W. Wu).

0013-7952/$ – see front matter © 2013 Elsevier B.V. All rights reserved.
http://dx.doi.org/10.1016/j.enggeo.2013.03.022

filling material type determines the specific fracture stiffness, which reflects a fracture mechanical property, and the wave transmission coefficient represents a fracture seismic property. Dry quartz sand was used to represent viscoelastic materials. The experimental investigation on the filled fracture was performed with various fracture properties and under different loading conditions, including fracture thickness, particle size of the filling sand, and loading rate of an incident wave. The experimental results are then compared with the analytical predictions by the DDM and the DSDM. This study lastly discusses the key fracture parameters in interrelating the physical, mechanical and seismic properties of a filled fracture.

2. Analytical models

In the DDM (Cai and Zhao, 2000), a rock fracture is considered as an interface between two elastic half-spaces with the same seismic impedance. When a normally incident P-wave propagates across a single rock fracture, the stresses across the fracture are continuous, whereas the displacements are discontinuous and equal to the stress divided by a constant normal specific stiffness

$$\begin{aligned} &\sigma^-(t) = \sigma^+(t) = \sigma(t) \\ &u^-(t) - u^+(t) = \frac{\sigma(t)}{k_n} \end{aligned} \tag{1}$$

where σ is the normal stress, u is the displacement along the normal direction, k_n denotes the specific fracture stiffness, which is the stress change per unit fracture closure, and the superscripts "−" and "+" denote the front and rear fracture interfaces, respectively.

The wave transmission coefficient for one-dimensional P-wave propagation across the fracture with linear deformation is described as

$$T_d = \frac{2\left(k_n/Z_p\omega\right)}{-i + 2\left(k_n/Z_p\omega\right)} \tag{2}$$

where i is the imaginary unit, Z_p is the seismic impedance of the rock material for the P-wave, which is the product of the rock density, ρ, and the longitudinal wave velocity, c, and ω is the wave angular frequency.

In the DSDM (Zhu et al., 2011), for a rock fracture filled with dry sand, the Kelvin model, consisting of one spring and one dashpot in parallel, can be adopted to describe the dynamic response of the filled fracture. The specific viscosity is set to zero for a fracture filled with dry sand. Thus the stress and displacement boundary conditions become

$$\begin{aligned} &\sigma^-(t) - \sigma^+(t) = -\omega^2 m_n u^+(t) \\ &u^-(t) - u^+(t) = \frac{\sigma^+(t)}{k_n} \end{aligned} \tag{3}$$

where the specific initial mass of the filling sand along the normal direction, m_n, is equal to the product of the sand density, ρ_s, and the initial thickness of the fracture, h. The specific initial mass is defined as the initial mass per unit area (i.e., the cross-section of the bars).

The wave transmission coefficient for the filled fracture can be written as

$$T_s = \frac{2}{2 - id_n - i/\left(k_n/Z_p\omega\right)} \tag{4}$$

where d_n is the impedance ratio between the filling sand and the rock material and expressed as

$$d_n = \frac{Z_e}{Z_p} = \frac{\omega m_n}{Z_p} = \frac{\omega\rho_s h}{Z_p} \tag{5}$$

where Z_e is the effective seismic impedance of the filling sand.

The calculation process of the DDM and DSDM predictions is shown in Fig. 1. The recorded incident wave in the time domain from an SHRB test is first transformed into the frequency domain by the fast Fourier transform (FFT). The derived wave transmission coefficient (i.e., T_d or T_s) multiplies the incident wave amplitude corresponding to each frequency to obtain the related transmitted wave amplitude. The transmitted wave amplitude is then transformed back to the time domain by the inverse fast Fourier transform (IFFT) to calculate the wave transmission coefficient. The wave transmission coefficient is defined as the ratio of the maximum strain of the transmitted wave to that of the corresponding incident wave in the time domain.

3. Experimental investigation

The experimental study was conducted using an SHRB apparatus (Fig. 2). Similar to a conventional SHPB, the apparatus consists of a pair of square norite bars with the cross-section of 40 mm × 40 mm and 1500 mm in length, a low-rate loading system with a striker bar with the same cross-section and 200 mm in length and a LabVIEW data acquisition unit for signal triggering, recording and storage. The high-quality norite material is an ideal material to study stress wave propagation due to the high density (i.e., 2900 kg/m^3), the high compressive strength (i.e., 284 MPa), a homogenous grain size and few visible cracks. In order to ensure that the bars have few defects that may influence stress wave propagation, the bars are carefully screened under an ultrasonic device. A spring with a stiffness coefficient of 9.52 N/mm is compressed as the energy source to instantaneously launch the striker bar at a low loading rate and to maintain elastic deformation of the bars during the test.

The one-dimensional wave propagation theory is applicable to square bars, if the lateral dimensions of the bars are much smaller than the wavelength (Kolsky, 1953). Two groups of strain gauges are mounted on each long bar, which are connected in the Wheatstone full-bridge to average out the bending strain and to reduce the signal noise. The strain gauge stations are 200 mm and 400 mm away from the fracture interfaces (the rear end of the incident bar and the front end of the transmitted bar). A rubber disc with 10 mm in diameter and 1 mm in thickness is employed as a pulse shaper. It is stuck at the impact end center of the incident bar to generate a non-dispersive low-rate loading pulse and to protect the contacting ends of the striker and incident bars.

As the half-wavelength of a generated sinusoidal pulse is 3000 mm, the short length of the incident and transmitted bars leads to the superposition of the positive and negative waves, which are denoted as waves along and opposite to the loading direction, respectively (Fig. 2). A wave separation method (Zhao and Gary, 1997) is adopted to separate the recorded signal into the positive and negative waves. The strain-time responses at the fracture interfaces can be calculated separately by time shifting the positive and negative waves at the strain gauge stations on each long bar. The stress–time responses at the front and rear interfaces of the filled fracture, $\sigma^-(t)$ and $\sigma^+(t)$, can then be determined by the Young's modulus of the norite, E, 63.6 GPa, multiplying the strain-time responses at the fracture interfaces on the incident and transmitted bars, $\varepsilon^-(t)$ and $\varepsilon^+(t)$, respectively

$$\begin{aligned} &\sigma^-(t) = E\varepsilon^-(t) = E\left(\varepsilon^{p-}(t) + \varepsilon^{n-}(t)\right) \\ &\sigma^+(t) = E\varepsilon^+(t) = E\left(\varepsilon^{p+}(t) + \varepsilon^{n+}(t)\right) \end{aligned} \tag{6}$$

where $\varepsilon^{p-}(t)$ and $\varepsilon^{p+}(t)$ are the positive waves at the front and rear interfaces, respectively, and $\varepsilon^{n-}(t)$ and $\varepsilon^{n+}(t)$ are the negative waves at the front and rear interfaces, respectively.

The fracture closure-time response, $\Delta u(t)$, can be obtained by the initial thickness of the filled fracture multiplying the strain-time response of the fracture, which is equal to the time integral of the difference of the

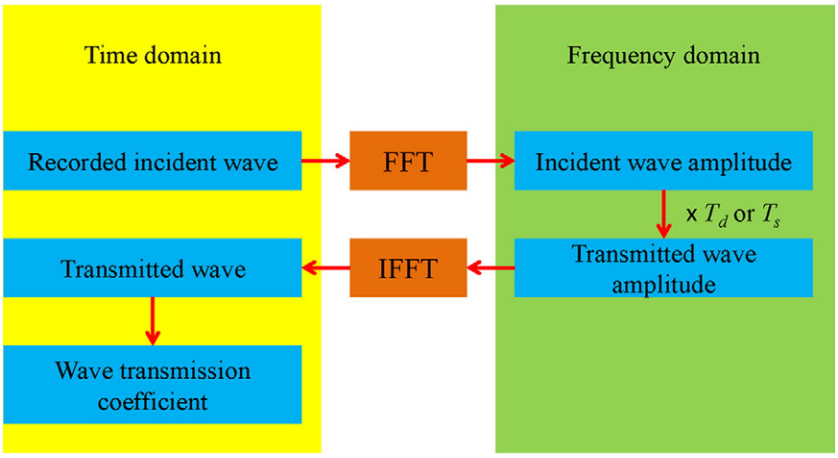

Fig. 1. The calculation process of the analytical predictions.

particle velocity-time responses at the front and rear interfaces, $v^-(t)$ and $v^+(t)$, respectively, over the initial thickness of the fracture

$$\begin{aligned}\Delta u(t) &= h \times \frac{1}{h}\int_0^t \left(v^-(t) - v^+(t)\right)dt \\ &= c\int_0^t \left[\left(\varepsilon^{p-}(t) - \varepsilon^{n-}(t)\right) - \left(\varepsilon^{p+}(t) - \varepsilon^{n+}(t)\right)\right]dt\end{aligned} \tag{7}$$

where c is the longitudinal wave velocity in the norite, 6000 m/s.

More details about the SHRB apparatus and the data analysis method can be obtained from Wu et al. (2012).

The validation test was performed on the SHRB system without the filling sand. Fig. 3 shows a successfully generated half-cycle sinusoidal pulse with a frequency of 2 kHz and the nearly identical stress–time responses at the front and rear interfaces during the first loading. Afterwards, the long bar ends lose the contact, which is not taken into account in the study. The dynamic stress equilibrium across the direct-contact interfaces indicates the integrity of the bars and the limited stress wave attenuation in the measuring range.

The filled fracture was simulated by filling the quartz sand with a particle density of 2620 kg/m^3 in a pre-set gap between the long bars. The quartz sand has a single mineral composition and zero viscosity under an air-dry condition. The quartz sand was sieved into three groups, coarse size (1–2 mm), medium size (0.5–1 mm) and fine size (0.25–0.5 mm). The initial porosity is determined by the volume of void space, V_0, over the volume of the sand layer, V

$$e_0 = \frac{V_0}{V} = \frac{V - V_s}{V} = \frac{V - m_n/\rho_s}{V} \tag{8}$$

where V_s is the volume of the quartz sand, which is equal to the initial mass, m_n, over the sand density, ρ_s. The volume of the sand layer is equal to the inner cross-section of the confining box multiplying the initial thickness of the fracture.

The filling sand was held by an aluminum box between the long bar ends to simulate the filled fracture. The inner cross-section of the confining box is 41 mm × 41 mm, the length is 20 mm and the thickness is 15 mm (Fig. 3 inset). A small grease layer was filled in the gap between the long bar surface and the box inner surface to reduce undesired friction. Fig. 3 also shows that the existence of the confining box does not obviously affect one-dimensional P-wave propagation across the direct-contact interfaces. All of the tests were conducted on a fracture filled with dry sand in a uniaxial strain state.

4. Results

Table 1 shows the experimental program on the dynamic response of a rock fracture filled with dry sand. Seven cases were investigated, and four tests were conducted for each case.

Fig. 4 shows the stress–time responses at the front and rear interfaces for various fracture thicknesses, such as 2 mm (Test No. 1-2), 4 mm (Test No. 2-1), and 8 mm (Test No. 3-2). Dynamic stress non-equilibrium across the filled fracture is observed. The stress–time response at the rear interface is clearly delayed and attenuated by the filling sand compared with that at the front interface. When the dynamic stress increases at the front interface, the uncompacted sand is compressed first, and then gradually transmits the incident energy to the rear interface. Felice et al. (1987) performed a series of SHPB tests on

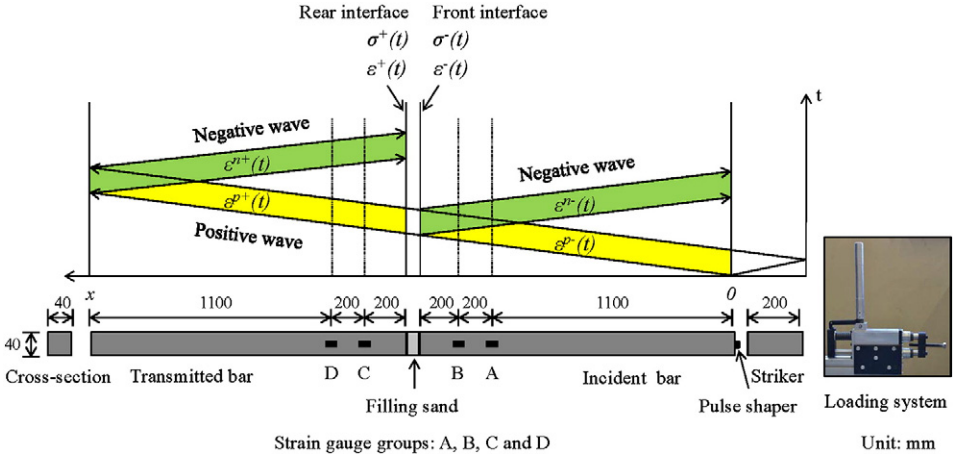

Fig. 2. Schematic view of the split Hopkinson rock bar and the x–t diagram of P-wave propagation in the system.

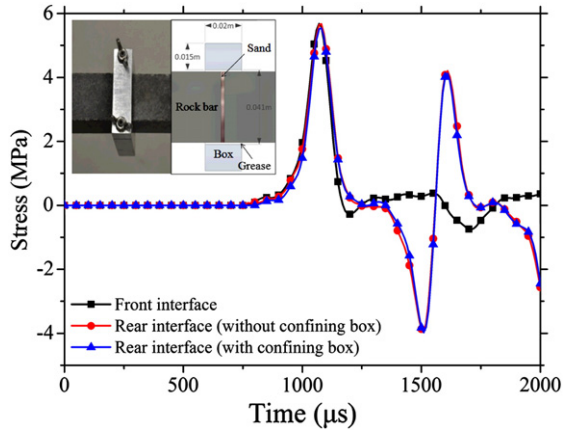

Fig. 3. Validation test and effect of the confining box on P-wave propagation in the system. The inset shows the photo and the schematic section of the confining box.

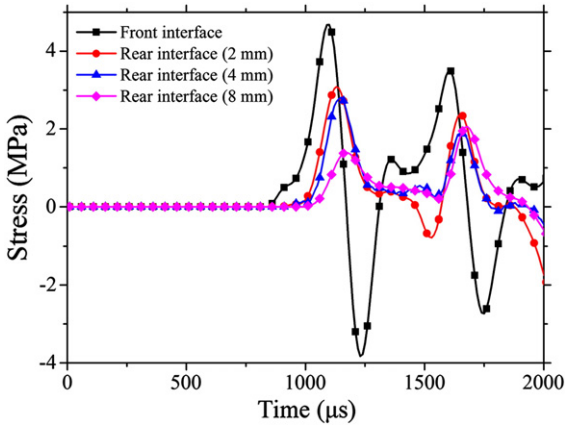

Fig. 4. Stress time histories of fracture interfaces (Tests No. 1-2, No. 2-1 and No. 3-2 as examples).

sand and found that when the compressive strain of the sand layer reaches its initial porosity, the sand layer can be in a stress equilibrium state. However, when the stress at the rear interface is rising and the void space is closing, the stress at the front interface in this test attains the maximum value and starts to decrease. The low loading rate impact limits the stress increase and the void closure. The dynamic compaction of the filling sand consumes a considerable amount of the incident energy and causes less energy to be transmitted through the filled fracture. Therefore, the dynamic stress non-equilibrium is mainly due to the existence of the filling sand, which delays the arrival time of the stress at the rear interface and consumes a considerable amount of the incident energy during the dynamic compaction.

In Fig. 5, the strains at the front and rear interfaces are discontinuous, where Test No. 2-1 is also taken as an example. The displacement discontinuity accounts for the stress discontinuity and the difference in the asperity deformation at the fracture interfaces. The P-wave induces different elastic deformation of asperities with uneven heights at the sawed unpolished surface (Fig. 5 inset). But the elastic deformation is quite small at the low stress levels due to the Young's modulus of the norite. It is evident that the compressive strain of the filling sand is about 1000 times larger than that of the fracture interfaces. Therefore, the closure of the fracture is dominated by the filling sand and the asperity deformation at the fracture interfaces can be neglected.

The complete stress–closure relation of a rock fracture filled with dry sand is shown in Fig. 6. The examples in Fig. 4 are used. The filled fracture exhibits a nearly linear stress–closure relation before the peak stress. When the quartz sand is filled in the fracture, the viscous property is restricted by the long bar ends and the confining box. The elastic property is responsible for wave transmission at the low stress levels. The specific fracture stiffness is defined as the slope of the tangent to the stress–closure curve. In this study, the specific fracture stiffness represents the normal stiffness of a filled fracture. The specific fracture stiffness decreases with increasing thickness of the filled fracture. The effects of fracture properties and loading conditions on the dynamic response of a filled fracture are discussed in the following section.

Table 1
Experimental program on dynamic response of a rock fracture filled with dry sand.

Experiments	Fracture thickness (mm)	Particle size (mm)	Number of tests	Loading rate (GPa/s)
1	2	1–2	4	40
2	4	1–2	4	40
3	8	1–2	4	40
4	4	0.5–1	4	40
5	4	0.25–0.5	4	40
6	4	1–2	4	30
7	4	1–2	4	60

Table 2 summarizes the analytical predictions based on the DDM and the DSDM and the experimental results. The predicted wave transmission coefficients by the DDM and the DSDM agree well. The analytical predictions of the wave transmission coefficients derived by the two models and the experimental results are close to each other. The wave transmission coefficient generally increases with increasing specific fracture stiffness. The difference between the two models in the description of the dynamic response of a filled fracture is further discussed below.

5. Discussion

The effects of fracture properties and loading conditions on the dynamic response of a rock fracture filled with dry sand are discussed in this section, including fracture thickness, particle size of the filling sand, and loading rate of an incident wave, based on the analytical predictions and the experimental results. This section also discusses the key fracture parameters in interrelating the physical, mechanical and seismic properties of a filled fracture.

5.1. Effect of fracture thickness

The thickness of the filling sand has a great effect on the dynamic response of a filled fracture. For a filled fracture with a smaller thickness (e.g. 2 mm, 4 mm, and 8 mm), as shown in the experimental results (Fig. 6), the fracture exhibits lower specific stiffness with increasing thickness. In Fig. 7, both analytical and experimental results show that

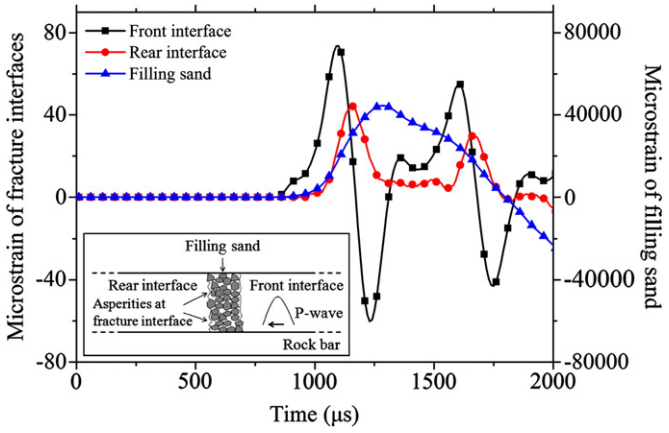

Fig. 5. Strain time histories of fracture interfaces and the filling sand (Test No. 2-1 as an example). The inset shows the schematic view of the filling sand and asperities at fracture interfaces.

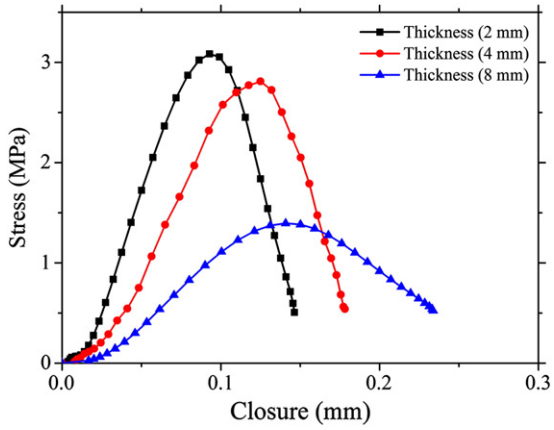

Fig. 6. Stress–closure relations of filled fractures with various thicknesses (Tests No. 1-2, No. 2-1 and No. 3-2 as examples).

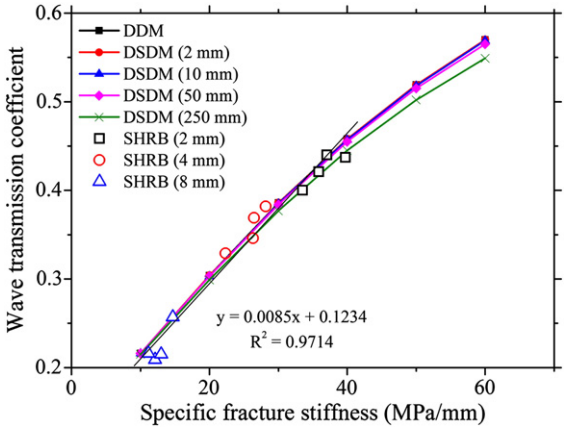

Fig. 7. Effect of fracture thickness and specific fracture stiffness on wave transmission coefficient.

the wave transmission coefficient increases with increasing specific fracture stiffness. The SHRB test is unable to generate a high-amplitude P-wave that propagates across a filled fracture with a larger thickness (e.g. larger than 50 mm), so the analysis for these cases is based on the analytical models. Fig. 7 also compares the analytical results of the DDM and the DSDM for a series of fracture thicknesses and various specific fracture stiffnesses. An incident wave with a loading rate of 40 GPa/s (Test No. 2-1) is used for this calculation. As mentioned above, the DSDM considers the specific initial mass of the filling sand, including the sand density and the fracture thickness, besides the parameters used in the DDM, i.e., the specific fracture stiffness, the seismic impedance of the rock material, and the wave angular frequency. For a fracture with a smaller thickness, e.g. 2 mm or 10 mm, the wave transmission coefficients predicted by the DDM and the DSDM match well for the specific fracture stiffness from 10 MPa/mm to 60 MPa/mm. The discrepancy is less than 0.5%. For a fracture with a larger thickness (e.g. 50 mm), the wave transmission coefficient predicted by the DSDM becomes smaller than that predicted by the DDM. The discrepancy increases from 0.3% for 20 MPa/mm to 0.5% for 30 MPa and to 0.9% for 60 MPa/mm. For a fracture with a thickness of 250 mm, the two models may not be able to describe the boundary conditions. The discrepancy of the wave transmission coefficients between the two models is larger than 1% when the specific fracture stiffness is larger than 20 MPa/mm. This is because the fracture thickness cannot be treated as a thin layer compared with the wavelength. This suggests that both the DDM and the DSDM can precisely describe a filled fracture with a smaller thickness (i.e., less than 10 mm), while the DSDM may be used to predict the dynamic response of a filled fracture with a larger thickness.

Table 2
Analytical predictions and experimental results of wave transmission coefficient as a function of specific fracture stiffness.

Experiment no.	Specific fracture stiffness (MPa/mm)	Wave transmission coefficient		
		Analytical prediction		Experimental result
		DDM	DSDM	
1-1	33.518	0.418	0.418	0.400
1-2	39.759	0.449	0.449	0.437
1-3	37.047	0.445	0.445	0.440
1-4	35.870	0.435	0.435	0.421
2-1	26.468	0.358	0.358	0.369
2-2	22.327	0.352	0.352	0.329
2-3	28.155	0.368	0.368	0.382
2-4	26.306	0.365	0.365	0.346
3-1	12.110	0.238	0.238	0.209
3-2	13.011	0.254	0.254	0.215
3-3	11.144	0.242	0.242	0.216
3-4	14.678	0.257	0.257	0.253
4-1	25.542	0.346	0.346	0.322
4-2	24.573	0.332	0.332	0.343
4-3	25.133	0.340	0.340	0.341
4-4	24.649	0.342	0.342	0.345
5-1	20.690	0.309	0.308	0.295
5-2	20.319	0.310	0.310	0.285
5-3	21.014	0.314	0.314	0.302
5-4	18.181	0.290	0.290	0.261
6-1	18.018	0.290	0.290	0.324
6-2	17.927	0.286	0.286	0.303
6-3	18.176	0.287	0.287	0.312
6-4	17.737	0.303	0.303	0.308
7-1	40.275	0.364	0.364	0.391
7-2	36.470	0.387	0.387	0.381
7-3	37.877	0.397	0.397	0.389
7-4	36.879	0.395	0.395	0.383

The wave transmission coefficient for a filled fracture with a larger thickness predicted by the DSDM is smaller than that predicted by the DDM, which is attributed to the filling sand compaction. A filled fracture with a larger thickness has more void space and more grain contacts. The sand compaction process in the filled fracture attenuates more incident energy and takes a longer time, because of the closure of void space and the friction between grain contacts. The transmitted waves at the rear interfaces thus show lower loading rates and lower amplitudes (Fig. 4). Therefore, stress wave attenuation in the filling sand must be taken into account for a filled fracture, besides the attenuation at the fracture interfaces. The attenuation becomes more obvious for a fracture with a larger thickness.

5.2. Effect of particle size

Fig. 8 shows the wave transmission coefficient as a function of the specific fracture stiffness for three particle sizes of the filling sand. The number next to each point is the initial porosity of the filling sand for the corresponding test. The experimental results indicate that a fracture filled with denser sand associated with finer particle size exhibits lower specific fracture stiffness and smaller wave transmission coefficient. A nearly linear relation between the wave transmission coefficient and the specific fracture stiffness is also observed.

For the low stress levels in this study (i.e., less than 3 MPa), the sand grains are considered under elastic deformation. The dynamic compaction induces grain contacts develop from a low stiffness at a small strain due to inter-particle contact to a high stiffness at a large strain due to packing densification (Cho et al., 2006). The coarser sand has a less number of grain contacts and higher stress per grain contact (Hagerty et al., 1993). The higher stress increases the contact stiffness between the sand grains and the global stiffness of the sand layer. On the contrary, the finer sand has lower contact stiffness because of more grain contacts and lower stress per grain contact. This discussion is based

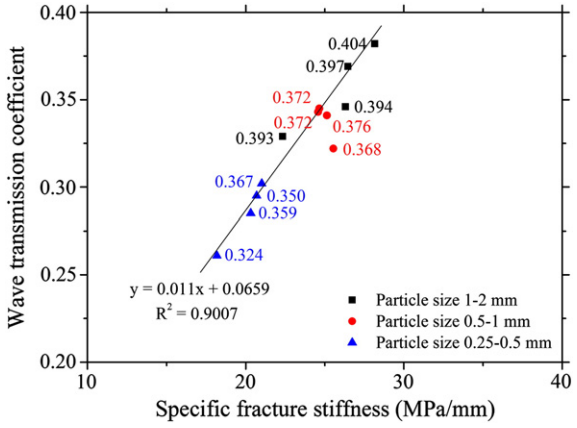

Fig. 8. Wave transmission coefficient as a function of specific fracture stiffness for a fracture filled with various sand particle sizes and the initial porosity of the filling sand corresponding to each point.

on the assumption that the sand grains are under elastic deformation at the low stress levels. The P-wave has a short loading duration and mainly induces instantaneous grain deformation, but restricts the sand grains to have long-time self-organization and fracturing as they do under static loading conditions. The grain fracturing is time consuming and reduces with increasing loading rate (Omidvar et al., 2012). Therefore, a fracture filled with coarser sand exhibits higher specific fracture stiffness and larger wave transmission coefficient at the stress levels.

5.3. Effect of loading rate

The wave transmission coefficient for a single non-welded contact fracture increases with increasing incident wave amplitude (Zhao et al., 2006a,b). Fig. 9 illuminates a similar trend for a fracture filled with dry sand. A P-wave with a higher loading rate exhibits larger amplitude and a shorter duration and induces higher specific fracture stiffness and larger wave transmission coefficient. Note that the linear deformational behavior is induced at the low stress levels, where the nonlinear normal deformation of the fracture is not considered.

An inhomogeneous contact network carries the dynamic load in the form of stress chains (Majmudar and Behringer, 2005). The loading rate effect on the dynamic response of the filled fracture is related to the effects of wave amplitude and loading duration on the formation of stress chains. (a) The incident energy (amplitude) increases with increasing loading rate. The higher incident energy induces a higher

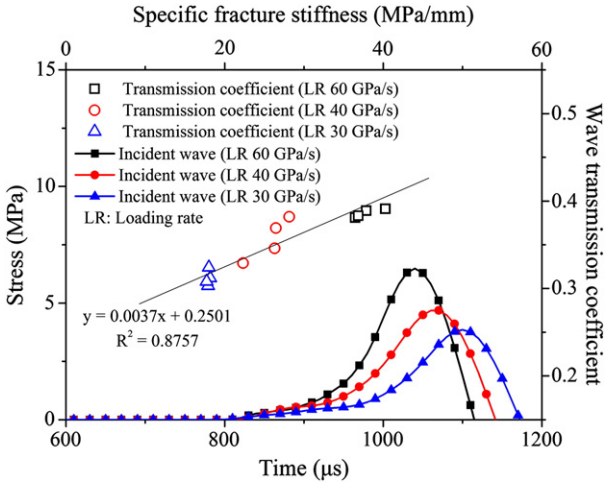

Fig. 9. Wave transmission coefficient as a function of specific fracture stiffness and the stress–time responses of P-wave under various loading rates.

stiffness between the sand grains and results in stronger stress chains for wave transmission. (2) The loading duration decreases with increasing loading rate. The short loading duration restricts grain arrangement and fracturing. Thus few stress chains are broken and the P-wave is less attenuated. The increase of the specific fracture stiffness under a higher loading rate is attributed to a better contact and seismic coupling of the sand grains in the filled fracture. Therefore, a higher loading rate induces higher wave amplitude and a short loading duration that assists to the formation of stress chains and promotes higher fracture stiffness and less wave attenuation.

5.4. Interrelations among filled fracture properties

According to the experimental results, the fracture properties and the loading conditions, such as the fracture thickness, the particle size of the filling sand, and the loading rate of an incident wave, are strongly related to the specific fracture stiffness. Pyrak-Nolte (1996) reported that the specific fracture stiffness is the key link of the interrelations among the physical, mechanical, and seismic properties of natural fractures, i.e., a non-welded contact fracture. The boundary conditions of the fracture are well described by the displacement discontinuity model. It is assumed that the fracture is plane, large in extent and small in thickness compared with the wavelength. The P-wave is attenuated due to wave reflection and transmission at the fracture interfaces. Nevertheless, for a fracture filled with viscoelastic materials, some characteristics are different from a non-welded contact fracture, for example, the specific initial mass of filling materials (including the density and the material thickness), the impedance jump between the rock medium and the filling materials (i.e., the wave velocity and the material density) and the increase in the fracture aperture (i.e., the distance between the front and rear interfaces). For a filled fracture with a larger thickness, the fracture thickness cannot be simply neglected compared with the wavelength and the filling material density is not negligible compared with the rock density. Eq. (3) shows that the stress discontinuity across a filled fracture is determined by the wave angular frequency and the specific initial mass of filling materials. Therefore, the displacement discontinuity model may be not appropriate to describe a filled fracture, in which the stress is discontinuous across the fracture.

Similar to a non-welded contact fracture, it is found that the specific fracture stiffness is also the key parameter of the interrelations among the physical, mechanical, and seismic properties of a fracture filled with dry sand. There is a nearly linear relation between the wave transmission coefficient and the specific fracture stiffness, as shown in Figs. 7–9. In addition, the specific initial mass of the filling sand is another key parameter to connect the physical and mechanical properties with the seismic property of the filled fracture. For example, the specific initial mass of the filling sand is related to the fracture thickness and the filling material type, which are related to the physical and mechanical properties, respectively. The two key parameters provide a precise description on the boundary conditions of the fracture and an exact prediction of the seismic property of the fracture. Stress wave attenuation in the filling sand is taken into account, besides the attenuation at the fracture interfaces. It is concluded that the specific fracture stiffness and the specific initial mass of the filling sand are two key parameters in interrelating the physical, mechanical and seismic properties of a fracture filled with dry sand. Note that this conclusion is based on a normally incident P-wave propagates across a single fracture filled with dry sand. Whether the conclusion is applicable to other cases, for instance, an oblique P-wave incidence, a fracture filled with saturated sand and a set of parallel fractures filled with viscoelastic materials, needs to be further investigated.

6. Conclusions

The dynamic response of a rock fracture filled with dry sand is analytically predicted by the DDM and the DSDM and experimentally investigated using an SHRB apparatus. It is verified that the specific

fracture stiffness and the specific initial mass of the filling sand are two key fracture parameters of the interrelations among the physical, mechanical and seismic properties of a filled fracture. A comparison between the analytical predictions and the experimental results shows that both the DDM and the DSDM can predict the dynamic response of a filled fracture with a smaller thickness (i.e., less than 10 mm). The DSDM may be applied to predict a fracture with a larger thickness by considering the specific initial mass of filling materials.

In general, the wave transmission coefficient increases with increasing specific fracture stiffness. Stress wave attenuation in a filled fracture is strongly affected by wave reflection and transmission at the fracture interfaces and the dynamic compaction of filling materials.

The SHRB test results exhibit that both stress and displacement are discontinuous over the filled fracture at the low stress levels. Although it is unable to reach high stress levels, the study extends current understanding of the dynamic response of a filled single fracture. The findings can be used to characterize the dynamic responses of a set of filled parallel fractures. Besides the dynamic compaction of filling materials, multiple wave reflections among fractures need to be considered for estimating the dynamic responses of filled parallel fractures. The analytical and experimental studies provide useful tools and reasonable parameters for numerical modeling on rock mass instability under the effect of seismic waves and dynamic loads. The understanding of the dynamic response of a filled fracture can also be used to interpret logging data from site investigation.

For some rock fractures filled with saturated sand or clay, or a liquid film, there may be some additional key parameters to be considered, such as the viscosity of filling materials and the hydraulic pressure. This is an area for the future study.

Acknowledgements

This work is sponsored by the Swiss National Science Foundation (200021_124846).

References

Cai, J.G., Zhao, J., 2000. Effect of multiple parallel fractures on apparent attenuation of stress waves in rock masses. International Journal of Rock Mechanics and Mining Sciences 37, 661–662.

Chen, W., Song, B., 2011. Split Hopkinson (Kolsky) Bar: Design, Testing and Applications. Springer, New York.

Cho, G.C., Dodds, J., Santamarina, J.C., 2006. Particle shape effects on packing density, stiffness, and strength: natural and crushed sands. Journal of Geotechnical and Geoenvironmental Engineering 132, 591–602.

Felice, C.W., Gaffney, E.S., Brown, J.A., Olsen, J.M., 1987. Dynamic high stress experiments on sand. Geotechnical Testing Journal 10, 192–202.

Hagerty, M.M., Hite, D.R., Ullrich, C.R., Hagerty, D.J., 1993. One-dimensional high-pressure compression of granular media. Journal of Geotechnical Engineering ASCE 119, 1–18.

Indraratna, B., Oliveira, D.A.F., Brown, E.T., 2010. A shear-displacement criteria for sand-infilled rock discontinuities. Geotechnique 60, 623–633.

Kolsky, H., 1953. Stress Waves in Solids. University Press, Oxford.

Leucci, G., Giorgi, D.L., 2006. Experimental studies on the effects of fracture on the P and S wave velocity propagation on sedimentary rock ("Calcarenite del Salento"). Engineering Geology 84, 130–142.

Li, J.C., Ma, G.W., 2009. Experimental study of stress wave propagation across a filled rock joint. International Journal of Rock Mechanics and Mining Sciences 46, 471–478.

Li, Y.X., Zhu, Z.M., 2012. Study on the velocity of P waves across a single joint based on fractal and damage theory. Engineering Geology 151, 82–88.

Majmudar, T.S., Behringer, R.P., 2005. Contact force measurements and stress-induced anisotropy in granular materials. Nature 435, 1079–1082.

Omidvar, M., Iskander, M., Bless, S., 2012. Stress–strain behavior of sand at high strain rates. International Journal of Impact Engineering 49, 192–213.

Pyrak-Nolte, L.J., 1996. The seismic response of fractures and the interrelations among fracture properties. International Journal of Rock Mechanics and Mining Sciences & Geomechanics Abstracts 33, 787–802.

Rokhlin, S.I., Wang, Y.J., 1991. Analysis of boundary conditions for elastic wave interaction with an interface between two solids. The Journal of the Acoustical Society of America 89, 503–515.

Schoenberg, M., 1980. Elastic wave behavior across linear slip interface. The Journal of the Acoustical Society of America 68, 1516–1521.

Wu, W., Zhang, W.D., Ma, G.W., 2010. Mechanical properties of copper slag reinforced concrete under dynamic compression. Construction and Building Materials 24, 910–917.

Wu, W., Li, J.C., Zhao, J., 2012. Loading rate dependency of dynamic responses of rock joints at low loading rate. Rock Mechanics and Rock Engineering 45, 421–426.

Wu, W., Zhu, J.B., Zhao, J., 2013. A further study on seismic response of a set of parallel rock fractures filled with viscoelastic materials. Geophysical Journal International 192, 671–675.

Zhao, J., 1997. Joint surface matching and shear strength, part a: joint matching coefficient (JMC). International Journal of Rock Mechanics and Mining Sciences 34, 173–178.

Zhao, H., Gary, G., 1997. A new method for the separation of waves: application to the SHPB technique for an unlimited duration of measurement. Journal of the Mechanics and Physics of Solids 45, 1185–1202.

Zhao, J., Cai, J.G., Zhao, X.B., Li, H.B., 2006a. Experimental study of ultrasonic wave attenuation across parallel fractures. Geomechanics and Geoengineering: An International Journal 1, 87–103.

Zhao, X.B., Zhao, J., Cai, J.G., 2006b. P-wave transmission across fractures with nonlinear deformational behavior. International Journal for Numerical and Analytical Methods in Geomechanics 30, 1097–1112.

Zhu, J.B., Perino, A., Zhao, G.F., Barla, G., Li, J.C., Ma, G.W., Zhao, J., 2011. Seismic response of a single and a set of filled joints of viscoelastic deformational behavior. Geophysical Journal International 186, 1315–1330.